Electron and ion distribution functions in RF and microwave plasmas

1995 Plasma Sources Sci. Technol. 4 172

(http://iopscience.iop.org/0963-0252/4/2/002)

Plasma Sources Sci. Technol. 4 (1995) 172–182. Printed in the UK

Electron and ion distribution functions in RF and microwave plasmas

U Kortshagen

Institute of Experimental Physics II, Ruhr-University Bochum, 44780 Bochum, Germany

Received 26 August 1994, in final form 8 November 1994

Abstract. Microwave and radio frequency (RF) sustained discharges play an important role in the field of plasma processing. For means of applications of microwave and RF plasmas the electron distribution function (EDF) in the plasma bulk and the ion energy distribution (IED) at the surrounding walls (electrodes or substrates) are equally important. In this paper a short review of the different effects governing EDFs and IEDs in microwave and RF plasmas is presented. Three aspects are treated in some detail: the differences of EDFs in DC and high-frequency sustained plasmas are pointed out. The spatial dependence of the EDF in low-pressure plasmas in the so called 'non-local regime' is investigated. Finally the different IEDs observed in capacitively and inductively coupled RF plasmas are discussed. For all three points theoretical as well as experimental results are presented.

1. Introduction

Microwave and radio frequency (RF) sustained plasmas (in the following also characterized as high-frequency (HF) plasmas) are nowadays widely used for technical applications, such as plasma etching, material deposition, sputtering, etc (see e.g. [1, 2]). For a thorough understanding of individual processes both the electron distribution function (EDF) in the plasma bulk and the ion energy distribution (IED) at the substrate to be processed are of high importance. The EDF in the plasma bulk determines the rates of electron induced reactions as ionization, excitation or dissociation. It therefore influences the macroscopic properties of the plasma such as the electron density profile or the distribution of particle fluxes (e.g. radicals) from the plasma. Thus, obviously not only the formation of the EDF in energy space but also its spatial dependence is of the utmost interest. The IED determines the rate of many plasma–surface interactions such as etching or sputtering. On the other hand damage of the materials is also connected to the IED, since it is induced by highly energetic ions.

Since the degree of ionization in many HF plasmas is rather low (about 10^{-6}–10^{-4}), electron–atom collisions can be much more effective in the formation of the EDF than electron–electron collisions, particularly in the energy range where inelastic collisions occur. It has been known for a long time now that this situation can lead to significantly non-thermal (non-Maxwellian) EDFs (e.g. [3–7]). The exact EDF has to be determined for every specific experimental situation and every background neutral gas. Even though it is not the intention of this paper to discuss all the effects which govern the formation of the EDF, two aspects should be treated in more detail—the influence of the HF electric field frequency on the formation of the EDF (section 2) and the spatial dependence of the EDF (section 3). A number of equally important aspects will only be mentioned briefly. For more information the reader is referred to the cited literature.

For the understanding of the formation of the IED, knowledge of the physical properties of the sheath in the considered HF plasma is necessary. It is well known, for instance, that totally different IEDs can be found in various RF plasmas. While in capacitively coupled RF plasmas at high input powers typical ion energies of several hundreds of eV can be found [8–12], in inductively coupled RF plasmas at the same or even higher power levels, ion impact energies of below 20 eV are possible [13, 14]. The understanding of this difference requires analysis of the sheaths and the processes responsible for the formation of the IED. A short survey of experimental and theoretical perceptions on this subject will be presented at the end of this paper in section 4.

For all the points mentioned above both theoretical as well as experimental results are presented. With regard to the theoretical approaches most of the results discussed here have been obtained using relatively simple models, mostly based on the solution of the Boltzmann equation with some approximations. It is one of the intentions of this paper to demonstrate that many effects can be understood and even quantitatively predicted by simple approaches. In modern discharge

0963-0252/95/020172+11$19.50

modelling very computer-intensive approaches (e.g. Monte Carlo based electron kinetics [15–17], PIC–MCC methods [18–23], convective scheme methods [24–27]) have been developed recently and represent very general methods to attack a wide variety of problems. However, in a number of situations simplifications can be applied without loss of accuracy. Simplified approaches can be much more efficient and may be even more transparent concerning the involved physical processes. With regard to the examples presented, it should also be stressed that it is worthwhile searching for simplified approaches to the description of electron and ion kinetics and checking these models directly with experiments. The application of simple, efficient self-consistent plasma models in direct connection to experiments can help to achieve a mutual stimulation of modelling and experiment. The value of more general models, however, should not be questioned, since they can always serve as a reference or guide for simpler models.

2. The influence of the HF field frequency

The influence of the EDF on the rates of various plasma processes has been discussed in a number of publications (e.g. [28–30]). For instance, changes in deposition rates have been observed on changing the field frequency [29]. These differences have tentatively been attributed to changes in the EDF. The frequency dependence of the EDF, however, has been known for some time. The first pioneering works concerning the EDF in microwave plasmas had already been performed in the late 1940s by Margenau [31], Margenau and Hartman [32]and MacDonald and Brown [33, 34]. Ferreira and Loureiro [35] pointed out the dependence of the EDF in argon plasmas on the ratio of the momentum transfer collision frequency to the field angular frequency ν_m/ω. Karoulina and Lebedev [36, 37] investigated the influence of the shape of the momentum transfer cross section on the EDF in microwave plasmas, which significantly affects the ν_m/ω ratio. A comparative experimental and theoretical analysis has also been given [38].

In figure 1 two typical EDFs for DC and microwave sustained plasmas in argon are depicted. Both EDFs differ significantly in the elastic range, i.e. for energies below the first excitation potential of 11.55 eV. While the EDF in the DC case shows a convex curvature in the elastic range, a concave curvature is observed in the microwave case. This obvious influence of the field frequency can be studied within a homogeneous plasma model. Such models have been used very successfully to study a number of effects which influence the formation of the EDF in energy space. Without claim of completeness, some important aspects should briefly be mentioned.

The starting point for homogeneous plasma models is usually the well known Boltzmann equation:

$$\frac{\partial F}{\partial t} + \nabla_r \cdot (vF) + \nabla_v \cdot (aF) = \left(\frac{\delta F}{\delta t}\right)_{\text{coll}} \qquad (1)$$

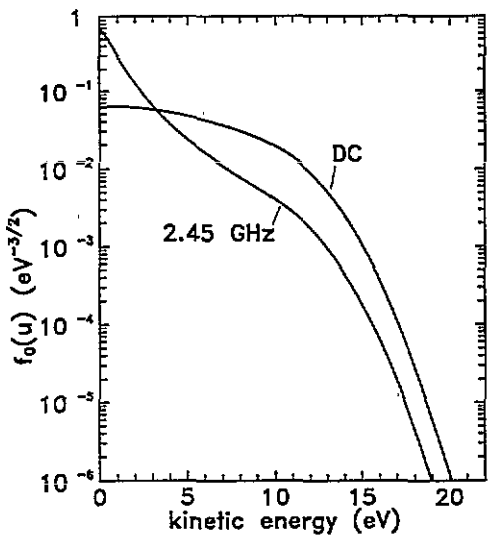

Figure 1. Typical EDFs in a microwave and a DC sustained plasma.

where the spatial dependence of the EDF is neglected, so that the ∇_r term cancels ('homogeneous' Boltzmann equation). $F(r, v, t)$ denotes the electron distribution function. A further simplification is achieved by the expansion of the EDF in spherical harmonics. A sufficiently isotropic EDF allows for the 'two-term expansion' into spherical harmonics (e.g. [39]):

$$F(v,t) \approx F_0(v,t) + \frac{v}{v} \cdot F_1(v,t). \qquad (2)$$

(When the kinetic energy is used instead of the velocity as the argument of F (see below), F_0 describes the energy distribution of chaotic, undirected motion, while the anisotropy component F_1 describes the directed motion.) The applicability of the two-term approximation has been the subject of a number of investigations, e.g. by Pitchford and Phelps [40] and by Braglia *et al* [41]. Comparisons have been performed to expansions including higher order spherical harmonics and to Monte Carlo calculations. As a result of these investigations, the two-term approximation has been shown to hold, if elastic collisions are frequent in comparison to inelastic ones, i.e. if $\nu_m \gg \nu^*$ (ν_m is the momentum transfer collision frequency, and ν^* is the total inelastic collision frequency). This inequality implies that the relaxation of directed motion (momentum) is much faster than the relaxation of the energy, which is contained in the chaotic motion.

For HF plasmas the potential time dependence of the EDF is also of interest. By numerical investigations covering a wide range of normalized frequencies ω/N_0 (N_0 is the neutral gas density) Winkler *et al* [42–44] pointed out that the ratio of the RF field angular frequency ω to the energy relaxation frequency

$$\nu_e(u) = \frac{2m_e}{M_a}\nu_m(u) + \nu^*(u) \qquad (3)$$

is the decisive parameter for the time dependence of the EDF. Here ν^* is the total inelastic collision frequency

and M_a is the atomic (or molecular) mass. The term comprising the momentum transfer collision frequency accounts for the energy relaxation in elastic collisions, which is small due to the very different masses of the scattering partners. For the case $\omega \gg \nu_e$ the field alteration is much faster than the energy relaxation, so that the isotropic part of the EDF F_0 (which describes the chaotic energy) becomes time independent. In this case the EDF is determined by some 'averaged' or effective field [45] (see below). In the limit $\omega \ll \nu_e$ the energy relaxation is faster than the field alteration and F_0 is strongly modulated in time. Since the elastic and inelastic contribution to ν_e differ usually by several orders of magnitude, both limiting cases can appear simultaneously at intermediate pressures or frequencies. In the energy range of elastic collisions $\omega \gg \nu_e$ can hold, while $\omega \ll \nu_e$ can apply in the range of inelastic collisions. Then F_0 is almost stationary in the elastic body of the EDF and strongly modulated in the inelastic tail [42].

The isotropic part of the EDF F_0 can therefore be expected to be time independent at sufficiently low pressures. On the other hand, in the homogeneous plasma approximation, the anisotropy component F_1 originates from the RF electric field $E(t) = E_0 e^{i\omega t}$ only [39], so that the EDF may be approximated as $F(v,t) \approx F_0(v) + v/v \cdot F_1(v) e^{i\omega t}$. Using these approximations and introducing the kinetic energy $u = m_e v^2/(2e)$ in volts leads to the well known, spatially homogeneous kinetic equation for the isotropic part of the EDF:

$$-\frac{d}{du}\left(u^{1/2} D_e(u) \frac{dF_0}{du} + V_e(u) F_0\right) = S_{ea} + S_{ee} \qquad (4)$$

with

$$u^{1/2} D_e = \frac{2e}{3m_e} \frac{u^{3/2}}{\nu_m} E_{eff}^2(u) \qquad (5)$$

$$E_{eff}^2 = \frac{E_0^2}{2} \frac{\nu_m^2(u)}{\omega^2 + \nu_m^2(u)} \qquad (6)$$

$$V_e = \frac{2m_e}{M_a} u^{3/2} \nu_m(u) \qquad (7)$$

$$S_{ea} = -\sum_k [\nu_k(u) F_0(u) u^{1/2} - \nu_k(u \pm u_k) \times F_0(u \pm u_k)(u \pm u_k)^{1/2}]. \qquad (8)$$

D_e is frequently named the energy diffusion coefficient, E_{eff} the effective field strength, and V_e describes the energy loss in elastic collisions. S_{ea} incorporates the removal and re-introduction of electrons from an energy element by inelastic processes. The plus signs in the second term of equation (8) account for excitation collisions with a threshold energy u_k, while the minus signs represent the related superelastic collisions. S_{ee} is the collision term describing electron–electron collisions (e.g. [46, 47]). This kinetic equation in the so called 'effective field approximation' has been the basis for a great number of investigations of the EDF in microwave plasmas. It demonstrates the dependencies of the EDF within the homogeneous plasma approximation: the EDF depends on the normalized field strength E_0/N (with N being the neutral gas density), on the ratio ν_m/ω and on the densities of molecules in the initial state of the kth process (via the collision frequencies ν_k). These states can be the ground state as well as excited states (electronically, vibrationally). For details on the action of excited states the reader is referred to the literature [48–57].

The different shapes of the EDFs in DC and microwave plasmas can be understood quite clearly by considering the effective field strength (equation (6)). (It is surely more correct to consider the behaviour of the energy diffusion coefficient. However, the result is essentially the same and the discussion of the effective field strength is more obvious.) The definition of E_{eff} accounts for the fact that the Joule heating of electrons is a collisional effect. If an electron moves without collisions in an HF field, its velocity is shifted in phase by $\pi/2$ compared to the electric field so that no heating occurs. For $\nu_m \ll \omega$ phase mixing collisions are seldom and heating is weak, since $E_{eff} \to E_0/\sqrt{2} \times \nu_m/\omega$. It can simply be shown that the optimal heating is achieved for $\nu_m = \omega$ [31]. In particular, for gases with a Ramsauer minimum in the momentum transfer cross section (e.g. argon), the condition $\nu_m \ll \omega$ may hold up to quite high pressures (or low HF frequencies) in the low-energy range. Electrons entering this energy range after having performed an inelastic scatter are only weakly heated and thus slowly removed from the low-energy interval. This effect leads to the observed overpopulation of the low-energy range (figure 2). In a DC field, on the other hand, low collision frequencies are even favourable for the heating of electrons. Electrons entering the low-energy range are very effectively removed by the DC electric field. Figure 2 clearly demonstrates the close correlation between the shape of the EDF in the microwave case and the energy dependence of the effective field strength. For growing energies, ν_m increases and, with it, so does E_{eff}. Electrons are heated more efficiently, causing an increase of the 'local temperature' $T_e = (d \ln F_0/du)^{-1}$ (note that the term 'local' is used for local in *energy space*).

Figure 3 shows two measured EDFs which have been determined by Langmuir probe measurements in surface wave produced plasmas. The experimental results agree well with the above considerations. The concave curvature of the EDF at 2.45 GHz and the expected low-energy peak are obvious. The EDF at 130 MHz resembles an EDF in a DC plasma, since $\nu_m > \omega$ holds for energies above 2.5 eV. In this case the effective field approaches $E_0/\sqrt{2}$ and becomes independent of ν_m/ω, exactly as in the DC case. For lower energies a small low-energy peak should be expected, which is, however, not resolved by the probe measurements.

Finally, it should be mentioned that the formation of a strong low-energy group can even be enhanced by other effects. In the capacitive RF discharge electron heating by the oscillating RF sheaths and secondary electrons have been pointed out by Godyak *et al* [60, 61]

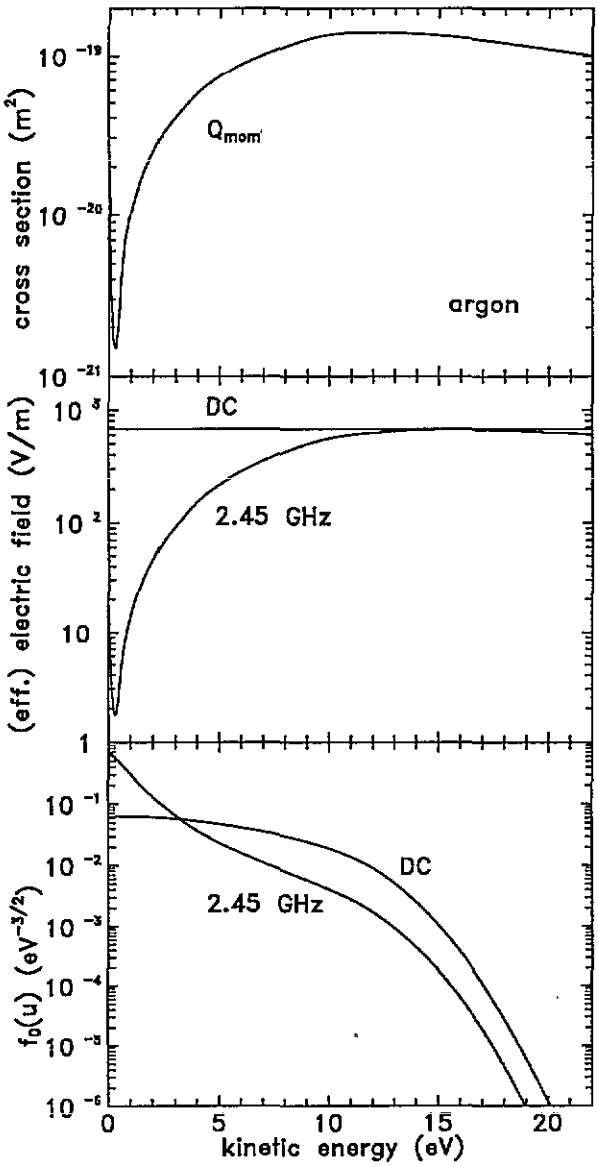

Figure 2. Relation between the energy dependence of the momentum transfer cross section, the effective electric field strength and the shape of the EDF in the low-energy part.

as reasons for very pronounced low-energy peaks in the EDF. Both effects lead to additional ionization, so that the energy input by Joule heating decreases. This leads to a lowering of the electric field in the bulk plasma. Since low-energy electrons are confined in this region by the space charge field (see below), they are heated less and their 'temperature' drops.

3. Influence of the spatial inhomogeneity

The influence of the spatial inhomogeneity of the EDF is of particular actual interest for mainly two reasons. The first is that historically most investigations of the electron kinetics have been performed on homogeneous plasma models so that the influence of the spatial inhomogeneity is up to now widely unexplored. The second is the need for the description of spatially inhomogeneous systems for modelling purposes.

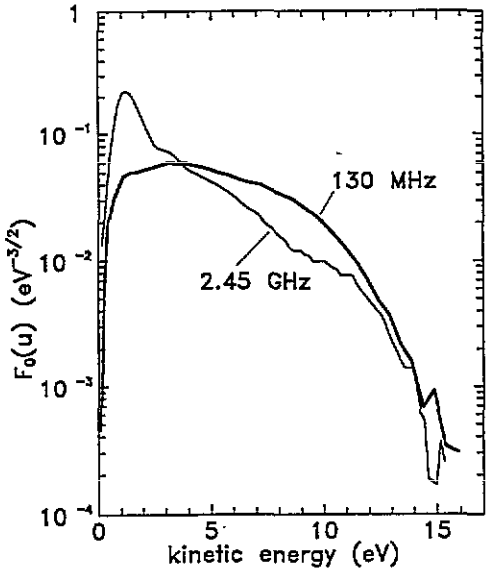

Figure 3. Measured EDFs in surface wave sustained argon plasmas. The EDF at 130 MHz has been measured at 450 mTorr and $R = 14$ mm, the EDF at 2450 GHz at 500 mTorr and $R = 15$ mm. (Measurements at 130 MHz from [58], at 2450 GHz from Grosse [59].)

Well established approaches to this problem are usually based on particle simulation techniques (e.g. particle in cell with Monte Carlo collisions (PIC–MCC) [18–23]) or on the numerical solution of the Boltzmann equation (e.g. the 'convective scheme' [24–27]). These methods are usually very computer intensive—even using modern computers, computation times of the order of several hours or days are frequently reported in the literature. This is probably one reason why many aspects of spatially inhomogeneous electron kinetics have not been thoroughly discussed until now. Another reason may be found in the fact that the above techniques are usually applied as one module between others in self-consistent plasma models so that the electron kinetics does not find particular attention in many investigations.

The fact that the treatment of the electron kinetics is frequently the most computer intensive part of self-consistent plasma models demonstrates the usefulness of the development of alternative techniques. The traditional method of solving the spatially dependent kinetic equation, which is obtained within the two-term approximation, is not so well established. Approaches to this problem have been reported in the literature [62–66]. (An approximate method by expansion into powers of the density gradient has been used for swarm experiments, e.g. [67–69].) The spatially dependent kinetic equation, which is obtained within this approach, is an elliptic partial differential equation. All approaches to solve this equation differ widely in the formulation of the boundary conditions, in particular at kinetic energy zero and at the discharge wall, so there is still much room for discussion. This method, however, seems to be very promising, since the numerical solution of the kinetic equations can be computed more efficiently than simulation techniques and may sometimes be even more physically transparent.

In approaches to the inhomogeneity problem, the space charge potential (or the related ambipolar, inhomogeneity electric field) appears as an additional complication in comparison to homogenous plasma models. Some authors have solved this problem in an elegant way by formulating the kinetic equations in *total energy* of the electrons rather than in velocity or kinetic energy [70]. The advantages will become evident below. If Φ is the potential related to the inhomogeneity (ambipolar) field $\boldsymbol{E}_t \| \nabla n_e$, the total energy ε in volts reads:

$$\varepsilon = u(r) - \Phi(r). \tag{9}$$

Usually Φ is counted negative with its zero in the maximum of the electron density. With this definition the spatially dependent kinetic equation for the isotropic part of the EDF takes the form of a diffusion equation in coordinate and energy space (here in cylindrical geometry):

$$\frac{1}{r}\frac{\partial}{\partial r}\left(rD_r(\varepsilon, r)u^{1/2}\frac{\partial F_0(\varepsilon, r)}{\partial r}\right) + \frac{\partial}{\partial \varepsilon}\left(D_e(\varepsilon, r)u^{1/2}\frac{\partial F_0(\varepsilon, r)}{\partial \varepsilon}\right) = S_{ea} + S_{ee}. \tag{10}$$

Since ε and r are used as independent coordinates, the kinetic energy $u(r) = \varepsilon - \Phi(r)$ is radially dependent. $D_r = 2e/3m_e \times u/\nu_m$ is the spatial diffusion coefficient, D_e is the energy diffusion coefficient (equation (5)) which incorporates E_{eff}^2.

The solution of this equation is still a complicated task. A simplification to the direct solution of this complete equation has been proposed by Bernstein and Holstein [70] and Tsendin [71]. Recently it has been demonstrated that their approach is a powerful tool for the accurate description of spatially inhomogeneous electron kinetics [72–75]. The main assumption of the so called 'non-local approach' is that the entire electron kinetics in a discharge is described by a single, spatially homogeneous EDF of total energy, which is determined from a spatially averaged equation. The *spatially resolved* EDF of kinetic energy is then determined by a 'modified Boltzmann relation'.

For electrons, which are confined in the space charge potential and move across the discharge without collisions and without being heated, this idea is obvious. The electrons move across the discharge with constant total energy. Thus the EDF of total energy is spatially constant: $F_0(\varepsilon, r) = F_0(\varepsilon)$. This situation should still hold in good approximations for the weakly collisional case, as long as the energy relaxation length $\lambda_\varepsilon \approx \lambda(\nu_m/\nu^*)^{1/2}$ exceeds the discharge dimensions, so that the total energy is still almost constant during the electron's spatial displacement. In argon, for instance, this imposes an upper limit for the applicability of $p\Lambda \approx 300$ mTorr cm (Λ is the typical inhomogeneity scale).

Experimental evidence for the existence of a spatially homogeneous EDF of total energy has been described in the literature. Probably the first demonstration was reported by Wiesemann [76], who interpreted his results as the experimental demonstration of the Barometric formula. Recently a very convincing qualitative demonstration of a spatially homogeneous EDF of total energy has been given by Godyak and Piejak [77] in a capacitively coupled RF plasma (figure 4(*a*)). The EDFs measured at different axial positions and plotted against the total energy coincide perfectly. (Note that the external probe voltage scale is exactly the total energy scale [73]. The zeros of the individual EDFs of kinetic energy are the points where the EDFs drop sharply at the low-energy side.) For a ten times higher pressure, when the total energy is no longer a constant of motion, they also demonstrated clear deviations from the homogeneity of F_0 (figure 4(*b*)).

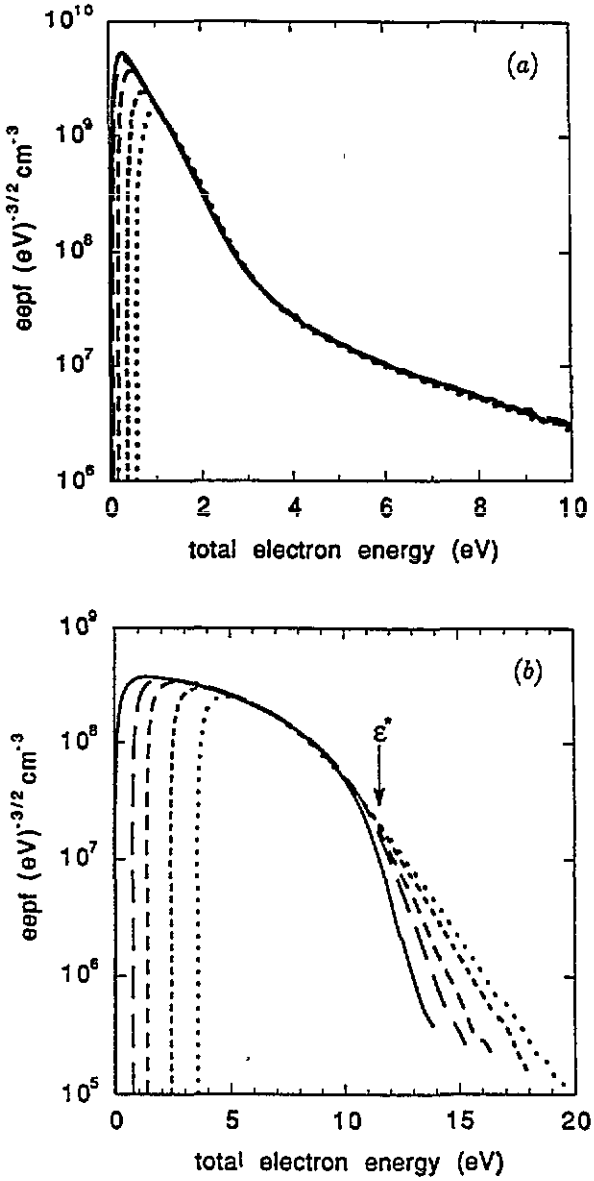

Figure 4. Axial evolution of the EDF in a capacitively coupled RF discharge in argon at $f = 13.56$ MHz and a gap width of 6.7 cm (reprinted with permission from Godyak and Piejak [77]). EDFs are shown in order of increasing distance from the midplane of the discharge: (*a*) $p = 0.03$ Torr, $x = 0.0$ (full), 7.5, 13.4, 19.6 and 22.5 mm; (*b*) $p = 0.3$ Torr, $x = 0.0$ (full), 13.4, 19.6, 25, 28.7 mm.

Figure 4(*a*) also demonstrates the relation between

the EDF of total energy and the individual EDFs of kinetic energy at different positions. Since the EDFs of kinetic energy are shifted according to the shift of the plasma potential, that part of the EDF of total energy with an energy less than the plasma potential at the probe position is always missing. These electrons are not able to reach this position and are confined to regions of lower potential energy. Thus the space charge potential at a distinct position cuts away the low-energy part of the EDF of total energy (by the amount of potential energy), and leaves the rest as the EDF of kinetic energy. This is, of course, the analogue of the Boltzmann relation for a non-Maxwellian EDF. The same concept is used in the non-local approach to determine the spatially resolved EDF of kinetic energy from the single EDF of total energy:

$$F_0(u, r) = F_0[\varepsilon = u - \Phi(r)]. \qquad (11)$$

Zero kinetic energy at the position r corresponds to the total energy $\varepsilon = -\Phi(r)$.

Within the non-local approach the spatially homogeneous EDF $F_0(\varepsilon)$ is determined from a spatially averaged kinetic equation. The justification for the averaging is that the spatial motion of electrons takes place much faster than their 'displacement' in energy space. Hence every point of the discharge cross section contributes to the formation of $F_0(\varepsilon)$ due to the fast spatial redistribution of obtained energy gains and losses. The resulting averaged equation looks formally the same as the spatially homogeneous kinetic equation:

$$\frac{\mathrm{d}}{\mathrm{d}\varepsilon}\overline{u^{1/2}D_e}(\varepsilon)\frac{\mathrm{d}F_0^{(0)}}{\mathrm{d}\varepsilon} = \overline{S_{ea}} + \overline{S_{ee}}. \qquad (12)$$

However, the bared quantities are spatially averaged coeffiecients, which are obtained by integrating equations (5)–(8) over the discharge cross section. The space charge potential Φ does not appear explicitly in equation (12) but it is hidden in the averaged coefficients.

While the existence of the EDF of total energy and the use of the 'modified Boltzmann relation' is quite clear, the use of a spatially averaged kinetic equation to determine $F_0(\varepsilon)$ has sometimes raised doubts or has been misunderstood. In order to support this concept it has been necessary to check it with experiments or by comparison to a more general method. A quantitative comparison between a self-consistent model, based on the non-local model, and measured EDFs in a surface wave discharge has been presented by Kortshagen [73]. There the non-local model for determining the EDF has been coupled to a fluid model for the ion dynamics and the solution of Maxwell's equations for the HF field. Rather good quantitative agreement between theory and measurements has been obtained (figure 5). With the quite simple self-consistent model it was possible to predict the radial variation of the EDF quantitatively correct.

It is a great advantage of the non-local approach that, regardless of the number of spatial dimensions to be considered, the electron kinetics is reduced to the solution of a one-dimensional, spatially averaged

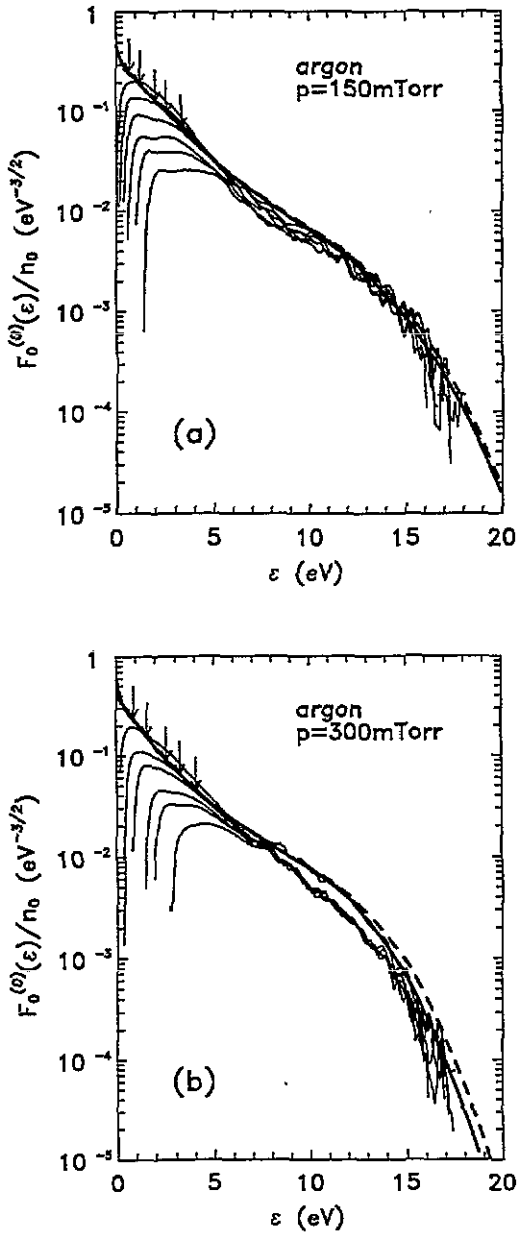

Figure 5. Comparison between radially resolved measurements of the EDF in an argon surface wave discharge and the results of a self-consistent model, based on the non-local approach. The full bold line represents the theoretical results with step-wise ionization, the broken curve the results without step-wise ionization accounted ((*a*) 150 mTorr, (*b*) 300 mTorr). The EDFs (from left to right) have been measured at r = 0, 6, 8, 10, 11 and 12 mm from the discharge axis (R = 14 mm). The arrows denote the theoretically determined values of the space charge potential at these positions (not given for r = 0 mm).

kinetic equation. This makes this approach very efficient for the description of multi-dimensional problems. Kortshagen and Tsendin [75] developed a (spatially) two-dimensional model for an inductively coupled plasma with a planar induction coil. Since these discharges are operated at low pressures of $\leqslant$ 10 mTorr, they are particularly favourable for the application of the non-local approach. Computation times of about 1 h on a 486 PC were achieved in comparison to computation times of the order of days on fast workstations otherwise. The theoretical results have been checked by radially

and axially resolved measurements of the EDF [74] and convincing agreement has been found. This success of the non-local approach is an illustrative example for the value of developing effective methods to describe the electron kinetics.

For highly collisional situations, when $\lambda_\varepsilon < \Lambda$, the correct solution of the spatially dependent kinetic equation (10) becomes inevitable. Figure 6 gives an example for results of a recently reported approach [65]. The EDF of total energy $F_0(\varepsilon, r)$ is plotted against total energy and radial position. In figure 6(a) the EDF shows the non-local behaviour, which has been discussed above, i.e. that $F_0(\varepsilon, r)$ is radially constant. The curved boundary at low energies represents the curve $\varepsilon = -\Phi(r)$ or $u(r) = 0$. Thus, obviously the EDFs of kinetic energy are not radially constant but are determined by the 'modified Boltzmann relation' (equation (11)). At higher pressures, considerable deviations from the radial constancy of F_0 arise in the energy range of inelastic processes. A strong depletion of the EDF towards the centre is visible, which is caused by the action of inelastic collisions. Since for a given total energy the kinetic energy is maximal in the centre, the efficiency of inelastic collisions is also maximal there. Therefore it is possible, for instance, that electrons which have a sufficiently high total energy to perform excitation close to the centre, are no longer able to perform this process close to the wall, where the kinetic energy (for given total energy) is smaller. So it is also not surprising that the boundary between elastic and inelastic range reflects the shape of the space charge potential, just shifted about the excitation energy. For energies higher than the wall potential (which has arbitrarily been fixed as $-\Phi_w = 18$ V in figure 6) a depletion of the EDF in the vicinity of the wall appears as well. This drop of the EDF is caused by the electron loss to the wall. For more details the reader is referred to reference [65]. A comparison between the non-local approach and the solution of the complete kinetic equation showed excellent quantitative agreements for normalized pressures up to 100 mTorr cm for argon.

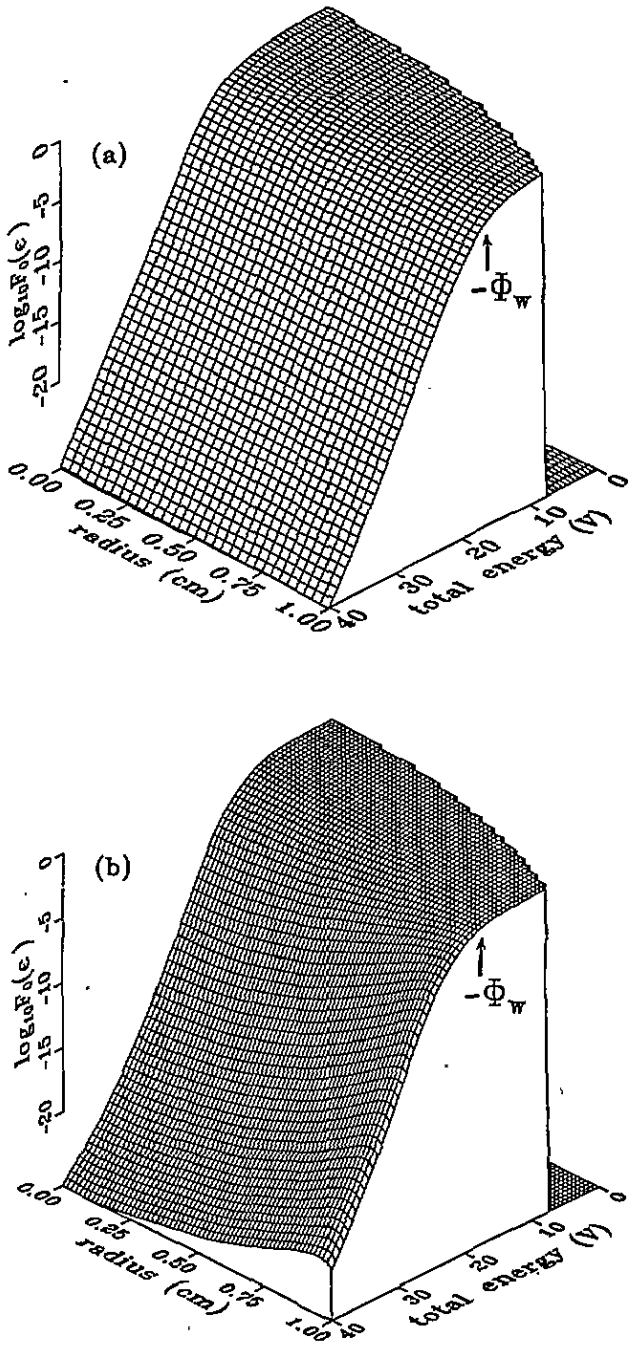

Figure 6. Numerical solutions of the spatially inhomogeneous kinetic equation for the isotropic part of the EDF. The calculations have been performed for the positive column (radially constant DC field) with $R = 1$ cm. For the lower neutral density $N_0 = 3 \times 10^{21}$ m^{-3} (a) the non-local behaviour is obvious, for the higher neutral density $N_0 = 3 \times 10^{23}$ m^{-3} (b) strong deviations from non-locality occur.

4. Ion energy distribution functions

The formation of the ion energy distribution is an important aspect for surface processing of materials. A recent trend in plasma etching is the search for discharge concepts, which provide high-density plasmas ($n_e > 10^{11}$ cm^{-3}) at simultaneously low and controllable ion energies, in order to avoid damaging the processed material by highly energetic ions [78]. A further requirement is excellent plasma homogeneity over a large planar area (e.g. a wafer) with a diameter of at least 20 cm. With the standard discharge for plasma etching, the capacitively coupled RF discharge at 13.56 MHz, this aim seems hardly achievable since high RF powers are connected to high sheath potentials across the RF sheaths. These potentials can be of the order of several hundreds of volts. Surendra and Graves [19] pointed out that lower ion energies at higher plasma densities may be achieved with the capacitive RF discharge by increasing the RF frequency above 13.56 MHz. Other concepts have been proposed, such as the helicon wave discharge [79, 80] or the electron cyclotron resonance discharge [81]. Recently, the low-pressure inductively coupled RF discharge has also attracted considerable interest [13, 14, 82–87]. Hopwood demonstrated that ion energies in this discharge are typically of the order of some 10 eV [13]. The differences between the IEDs

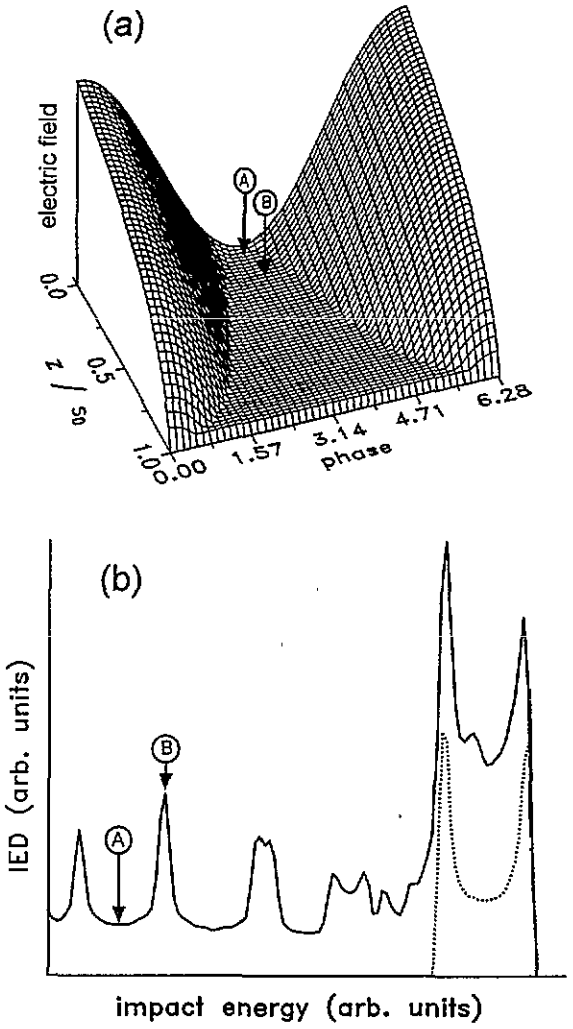

Figure 7. Scheme for the formation of the IED in the collisional sheath of a capacitive RF discharge: (*a*) schematic temporal evolution of the electric field; (*b*) time-averaged IED. The dotted curve represents the contribution of ions, which have passed the whole sheath without collisions. For point B the condition $dE_{impact}/dz = 0$ holds, for point A it does not.

in the capacitively and inductively coupled discharge are, of course, connected to the different natures of the sheaths in these discharges.

A RF sheath, to which high RF potentials are applied, is found in capacitively coupled RF discharges. In discharges in electropositive gases almost the whole applied RF voltage drops across both sheaths. Since the sheath voltage is strongly modulated in time the sheath thickness also varies periodically between a maximum value, which is at least roughly given by the Child-Langmuir law, and a minimum value (see figure 7(*a*)). This minimum thickness is assumed to be zero in simple analytic models [88, 89]. In more sophisticated models it is of the order of a few Debye lengths [90, 91].

The formation of the IED at the electrode is crucially determined by the ratio of the ion transit time through the sheath τ to the RF period $T = 2\pi/\omega$. For $\tau \gg T$ the ions are only affected by the time-averaged electric field. The IED is time independent and in the case of a collisionless sheath has a monoenergetic peak. For decreasing τ/T the ion impact energy starts to depend on the entrance phase of the ions into the sheath. The single monoenergetic peak forming the IED (still collisionless case) now oscillates periodically along the energy axis. However, usually only the time-averaged IED is observed experimentally. For the understanding of the time-averaged IED it is important to note that the oscillating peak stays at the turning points of its motion along the energy axis, i.e. the maximal and minimal energy, for a longer time than at energies between them. This behaviour leads to the typical saddle-like double peak structure (dotted curve in figure 7(*b*)), as was first pointed out by Tsui [92]. In collisional sheaths an additional structure appears—at lower energies than those of the plasma saddle structure—which was first investigated experimentally and theoretically by Wild and Koidl [10, 93] (see also [94]). An interpretation for this structure has been given by Biehler on the basis of the time-resolved IED [91]. The structure stems from thermal ions, which are 'born' in the sheath region due to charge exchange collisions. Their production rate is approximately constant in time due to the constant flux of ions coming from the plasma. The ions which are generated in the low-field phase are only weakly accelerated and remain (almost) stationary until the high sheath field returns (see figure 7(*a*)). Then a 'bunch' of ions starts to travel to the electrode. The ions coming from different generation positions reach the electrode at different times usually with different energies. In the time-resolved IED they again form a monoenergetic peak, which moves along the energy axis as the time proceeds. Peaks in the time-averaged IED are only observed at energies, where the motion of the peak (along the energy axis) stops for some time, i.e. where $dE_{impact}/dt = 0$. Note that this criterion is equivalent to the criterion $dE_{impact}/dz = 0$ (z = start position in the sheath) derived by Wild and Koidl [93].

Hopwood [13] pointed out that the IEDs in the inductively coupled RF discharge possess much lower ion energies than in the capacitive discharge. In an inductively coupled RF discharge, no RF potential is applied to the sheath since the induction electric field is not connected to a potential. Some parasitic capacitive coupling from the induction coil is possible, which becomes unimportant for high electron densities due to screening by the plasma. At low electron densities screening by a Faraday shield may be necessary to realize a purely inductive coupling. In this case ion energies of below 20 eV are obtained (figure 8) [95]. The IEDs can be interpreted as distributions which are formed in the collisional presheath and which are then accelerated in the collisionless sheath. The sheath can be considered collisionless, since its extension is only a few Debye lengths if all capacitive couplings are avoided. The problem of the IED formation in the presheath has been discussed by Riemann [96]. What remains to be determined is the potential drop within the sheath. One alternative is the use of the well known formula from the probe theory, which describes the difference between the plasma potential and a floating probe [97]:

$$\Delta\Phi_{sh} = \frac{kT_e}{e} \ln\left(\frac{M_a}{m_e}\right)^{1/2}. \qquad (13)$$

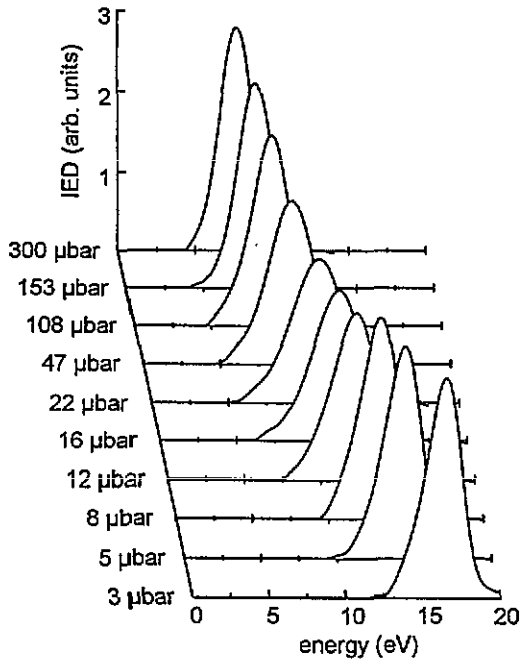

Figure 8. IEDs measured in an inductively coupled discharge. An electrostatic screen has been used to avoid parasitic capacitive coupling (from [95]).

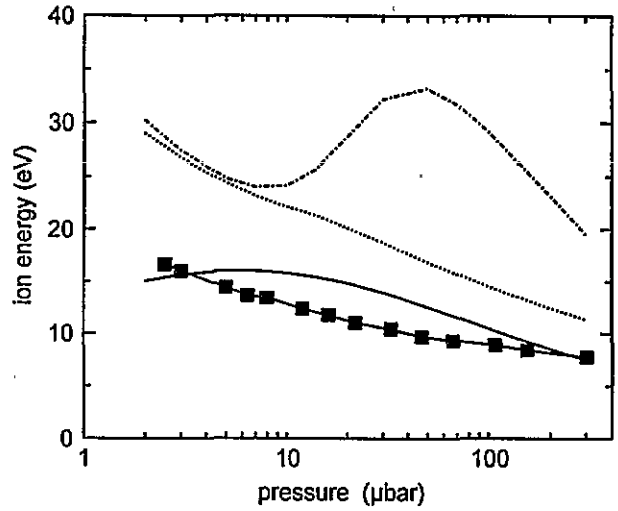

Figure 9. Measured and calculated ion energies for the inductive discharge with purely inductive coupling. The symbols represent the measurements, the full curve represents ion energies obtained from a non-local plasma model. The other curves represent ion energies obtained from equation (13), using $kT_e = 2/3 \times \langle u \rangle$ (dotted curves) or the 'screening temperature' $kT_e = (\mathrm{d} \ln n_e / \mathrm{d}\Phi)^{-1}$ (from [95]).

This formula relies on the assumption of a Maxwellian EDF. Since the real EDF is non-Maxwellian, a temperature kT_e has to be defined. For comparison to the experiment, the frequently used definition by the mean energy $kT_e/e = 2/3 \times \langle u \rangle|_{sb}$ (sb represents the sheath boundary) as well as the so called 'screening temperature' $kT_e/e = (\mathrm{d} \ln n_e / d\Phi)^{-1}$ [98] have been used. However, as is demonstrated by figure 9, equation (13) does not reproduce the experiment properly. Due to the assumption of a Maxwellian the population of the high-energy tail of the EDF is overestimated, which results in too high sheath potentials in order to repel the high-energy electrons. A better estimate can be found from the consideration of the actual non-thermal EDF, as has been recently demonstrated [95]. Following the idea of non-locality of the EDF, the wall potential can be estimated from the following consideration [99]: electrons with a total energy exceeding the (negative) wall potential are lost from the plasma with high probability. From $F_0(\varepsilon)$ and the space charge potential the total ionization, as well as the total number of wall losses, can be determined. In particular the wall loss rate depends significantly on the wall potential. Thus the wall potential has to adjust itself to balance the wall losses to the total ionization in the discharge. The potential at the plasma–sheath transition can approximately be found from an ion fluid approach. The sheath potentials, which are found from this consideration, agree much better with the experimental ion energies than the results of equation (13). For a more detailed presentation the reader is referred to reference [95].

Finally it should be noted that a remaining capacitive coupling in the inductive discharge is very sensitively observed at the IEDs. The IEDs then show similar features as in the capacitive discharge. By applying a small RF voltage to the electrode (wafer), this effect can be used to achieve controllable self-bias voltages and thus to control the ion impact energy [14].

5. Summary and conclusions

In this paper a short survey of the different effects governing the electron kinetics in microwave and RF plasmas has been given. Examples for combined experimental and theoretical investigations, using simple kinetic models, have been presented. Three aspects have been considered in detail. The shape of the EDF at different frequencies has been related to the ratio ν_m/ω, which is decisive for the efficiency of the collisional heating. The higher the efficiency of the collisional heating, the higher the local temperature of the EDF. It has been demonstrated that the spatial dependence of the EDF can be well understood with use of the non-local model. Quantitative agreement between measured EDFs and non-local kinetic models has been pointed out. By comparisons with a more sophisticated numerical model it has been shown that the non-local regime extends to normalized pressures $pR < 100$ mTorr cm in argon. At higher pressures deviations from the spatial homogeneity of $F_0(\varepsilon, r)$ appear which can be attributed to inelastic collisions and wall losses. Furthermore, the differences of IEDs behind sheaths with and without applied RF potential have been pointed out. In capacitively coupled RF discharges, where the former case is met, very high ion energies can be obtained. Due to the large sheath thickness, collisional effects can influence the formation of the IED. In inductively coupled RF discharges (no RF potential across the sheath) ion energies of below 20 eV

are found. These can be explained by the consideration of the actual non-thermal EDF.

It has been stressed that the search for efficient, simple models for the description of the spatially inhomogeneous electron kinetics is an important task for the further development of plasma modelling. The non-local model is such an approach and its advantages compared to simulation techniques are obvious. Its applicability, however, is restricted to weakly collisional plasmas. For molecular gases with low threshold energies for vibrational excitation the applicability may be even more limited. In these systems the present modelling approaches (e.g. by simulation techniques) seem to work fairly well, even at the expenses of computation time. However, the development of more efficient approaches to these systems seems to be desirable.

Acknowledgments

The author is grateful to Professor H Schlüter for valuable discussions and for the support of his work. He is thankful to Dr K-U Riemann for carefully reading the manuscript and for valuable discussion. The author thanks C Busch, S Grosse and Dr M Zethoff for contributing materials prior to publication. This work was supported by the Deutsche Forschungsgemeinschaft (SFB 191).

References

[1] Chapman B N 1980 *Glow Discharge Processes* (New York: Wiley)
[2] Graves D B 1994 *IEEE Trans. Plasma Sci.* **22** 31
[3] Allis W P 1956 *Handbuch der Physik* vol 21, ed S Flügge (Berlin: Springer) p 383
[4] Kagan Y M and Lyagushchenko R I 1961 *Sov. Phys.–Tech. Phys.* **6** 321
[5] Kagan Y M and Lyagushchenko R I 1962 *Sov. Phys.–Tech. Phys.* **7** 134
[6] Holstein T 1946 *Phys. Rev.* **70** 367
[7] Winkler R 1973 *Ann. Phys.* **29** 37
[8] Coburn J W and Kay E 1972 *J. Appl. Phys.* **43** 4965
[9] Kuypers A D and Hopman H J 1988 *J. Appl. Phys.* **63** 1894
[10] Wild C and Koidl P 1989 *Appl. Phys. Lett.* **54** 505
[11] Manenschijn A, Janssen G C M, van der Drift E and Radelaar S 1991 *J. Appl. Phys.* **69** 1253
[12] Flender U and Wiesemann K 1994 *J. Phys. D: Appl. Phys.* **27** 509
[13] Hopwood J 1993 *Appl. Phys. Lett.* **62** 940
[14] Keller J H, Forster J C and Barnes M S 1993 *J. Vac. Sci. Technol.* A **11** 2487
[15] Kushner M J 1983 *J. Appl. Phys.* **54** 4958
[16] Kushner M J 1987 *J. Appl. Phys.* **61** 2784
[17] Sommerer T J and Kushner M J 1992 *J. Appl. Phys.* **71** 1654
[18] Surendra M, Graves D B and Morey I J 1990 *Appl. Phys. Lett.* **56** 1022
[19] Surendra M and Graves D B 1991 *Appl. Phys. Lett.* **59** 2091
[20] Boswell R W and Morey I J 1988 *Appl. Phys. Lett.* **52** 21
[21] Vahedi V, Birdsall C K, Liebermann M A, DiPeso G and Rognlien T D 1993 *Phys. Fluids* B **5** 2719
[22] Vahedi V, DiPeso G, Birdsall C K, Liebermann M A and Rognlien T D 1993 *Plasma Sources Sci. Technol.* **2** 261
[23] Vahedi V, Birdsall C K, Liebermann M A, DiPeso G and Rognlien T D 1993 *Plasma Sources Sci. Technol.* **2** 273
[24] Hitchon W N G, Koch D J and Adams J B 1989 *J. Comput. Phys.* **83** 79
[25] Sommerer T J, Hitchon W N G and Lawler J E 1989 *Phys. Rev. Lett.* **63** 2361
[26] Sommerer T J, Hitchon W N G and Lawler J E 1989 *Phys. Rev.* A **39** 6356
[27] Hitchon W N G, Parker G J and Lawler J E 1993 *IEEE Trans. Plasma Sci.* **21** 228
[28] Flamm D L 1986 *J. Vac. Sci. Technol.* A **4** 729
[29] Wertheimer M R and Moisan M 1985 *J. Vac. Sci. Technol.* A **3** 2643
[30] Moisan M, Barbeau C, Claude R, Ferreira C M, Margot J, Paraszczak J, Sá A B, Sauvé G and Wertheimer R 1991 *J. Vac. Sci. Technol.* B **9** 8
[31] Margenau H 1948 *Phys. Rev.* **73** 297
[32] Margenau H and Hartmann L M 1948 *Phys. Rev.* **73** 309
[33] MacDonald A D and Brown S C 1949 *Phys. Rev.* **75** 411
[34] MacDonald A D and Brown S C 1949 *Phys. Rev.* **76** 1634
[35] Ferreira C M and Loureiro J 1983 *J. Phys. D: Appl. Phys.* **16** 2471
[36] Karoulina E V and Lebedev Y A 1988 *J. Phys. D: Appl. Phys.* **21** 411
[37] Karoulina E V and Lebedev Y A 1992 *J. Phys. D: Appl. Phys.* **25** 401
[38] Kortshagen U 1993 *J. Phys. D: Appl. Phys.* **26** 1230
[39] Shkarofsky I P, Johnston T W and Bachynski M P 1966 *The Particle Kinetics of Plasmas* (Reading, MA: Addison-Wesley)
[40] Pitchford L C and Phelps A V 1982 *Phys. Rev.* A **25** 540
[41] Braglia G L, Wilhelm J and Winkler R 1985 *Lett. Nuovo Cimento* **44** 365
[42] Winkler R, Deutsch H, Wilhelm J and Wilke C 1984 *Beitr. Plasmaphys.* **24** 285
[43] Winkler R, Wilhelm J and Hess A 1985 *Ann. Phys.* **42** 537
[44] Winkler R, Dilonardo M, Capitelli M and Wilhelm J 1987 *Plasma Chem. Plasma Proc.* **7** 125
[45] Winkler R, Deutsch H, Wilhelm J and Wilke C 1984 *Beitr. Plasmaphys.* **24** 303
[46] Dreicer H 1960 *Phys. Rev.* **117** 343
[47] Schlie L A 1976 *J. Appl. Phys.* **47** 1397
[48] Alves L A, Gousset A and Ferreira C M 1992 *J. Phys. D: Appl. Phys.* **25** 1713
[49] Ferreira C M, Loureiro J and Ricard A 1985 *J. Appl. Phys.* **57** 82
[50] Gorse C, Bretagne J and Capitelli M 1988 *Phys. Lett.* **126A** 277
[51] Gorse C, Capitelli M, Longo S, Estocq E and Bretangne J 1991 *J. Phys. D: Appl. Phys.* **24** 1947
[52] Vlček J 1989 *J. Phys. D: Appl. Phys.* **22** 623
[53] Vlček J and Pelikán V 1989 *J. Phys. D: Appl. Phys.* **22** 632
[54] Capriati G, Boeuf J P and Capitelli M 1993 *Plasma Chem. Plasma Proc.* **13** 499
[55] Longo S and Capitelli M 1994 *Phys. Rev.* E **49** 2302
[56] Capitelli M, Gorse C, Winkler R and Wilhelm J 1987 *J. Appl. Phys.* **62** 4398
[57] Capitelli M, Celiberto R, Gorse C, Winkler R and Wilhelm J 1988 *J. Phys. D: Appl. Phys.* **21** 691
[58] Böhle A and Kortshagen U 1994 *Plasma Sources Sci. Technol.* **3** 80
[59] Grosse S private communication
[60] Godyak V A, Piejak R B and Alexandovich B M 1992 *Phys. Rev. Lett.* **68** 40
[61] Godyak V A, Piejak R B and Alexandrovich B M 1992 *Plasma Sources Sci. Technol.* **1** 36
[62] Feoktistov V A, Popov A M, Popovicheva O B, Rakhimov A T, Rakhimova T V and Volkova E A 1991 *IEEE Trans. Plasma Sci.* **19** 163

[63] Meijer P M, Goedheer W J and Passchier J D P 1992 *Phys. Rev.* A **45** 1098
[64] Hartig M J and Kushner M J 1993 *J. Appl. Phys.* **73** 1080
[65] Busch C and Kortshagen U 1995 *Phys. Rev.* E **51** 280
[66] Uhrlandt D and Winkler R 1994 *Proc. 12th Eur. Sectional Conf. on the Atomic and Molecurlar Physics of Ionized Gases* ed M C M V de Sanden (European Physical Society)
[67] Skullerud H R 1969 *J. Phys. B: At. Mol. Phys.* **2** 696
[68] Parker J H Jr and Lowke J J 1969 *Phys. Rev.* **181** 290
[69] Pitchford L C, O'Neil S V and Rumble J R Jr 1981 *Phys. Rev.* A **23** 294
[70] Bernstein I B and Holstein T 1954 *Phys. Rev.* **94** 1475
[71] Tsendin L D 1974 *Sov. Phys.-JETP* **39** 805
[72] Kaganovich I D and Tsendin L D 1992 *IEEE Trans. Plasma Sci.* **20** 66
[73] Kortshagen U 1994 *Phys. Rev.* E **49** 4369
[74] Kortshagen U, Pukropski I and Zethoff M 1994 *J. Appl. Phys.* **76** 2048
[75] Kortshagen U and Tsendin L D 1994 *Appl. Phys. Lett.* **65** 1355
[76] Wiesemann K 1969 *Ann. Phys. Lpz* **23** 275
[77] Godyak V A and Piejak R B 1993 *Appl. Phys. Lett.* **63** 3137
[78] Hopwood J 1992 *Plasma Sources Sci. Technol.* **1** 109
[79] Boswell R W and Porteous R K 1987 *Appl. Phys. Lett.* **50** 1130
[80] Chen F 1991 *Plasma Phys. Control. Fusion* **33** 339
[81] Asmussen J 1989 *J. Vac. Sci. Technol.* A **7** 883
[82] Barnes M S, Forster J C and Keller J H 1993 *Appl. Phys. Lett.* **62** 2622
[83] Carter J B, Holland J P, Peltzer E, Richardson B, Nguyen H T, Melaku Y, Gates D and Ben-Dor M 1993 *J. Vac. Sci. Technol.* A **11** 1301
[84] Hopwood J, Guarnieri C R, Whitehair S J and Cuomo J J 1993 *J. Vac. Sci. Technol.* A **11** 152
[85] Patrick R, Schoenborn P, Toda H and Bose F 1993 *J. Vac. Sci. Technol.* A **11** 1296
[86] Ventzek P L G, Hoekstra R J and Kushner M J 1994 *J. Vac. Sci. Technol.* B **12** 461
[87] Stewart R A, Vitello P and Graves D B 1994 *J. Vac. Sci. Technol.* B **12** 478
[88] Lieberman M A 1988 *IEEE Trans. Plasma Sci.* **16** 638
[89] Lieberman M A 1989 *IEEE Trans. Plasma Sci.* **17** 338
[90] Godyak V A and Sternberg N 1990 *Phys. Rev.* A **42** 2299
[91] Biehler 1991 *PhD Thesis* University Bochum (in German)
[92] Tsui R T C 1968 *Phys. Rev.* **168** 107
[93] Wild C and Koidl P 1991 *J. Appl. Phys.* **69** 2909
[94] Manenschijn A and Goedheer W J 1991 *J. Appl. Phys.* **69** 2923
[95] Kortshagen U and Zethoff M 1995 *Plasma Sources Sci. Technol.* submitted
[96] Riemann K-U 1981 *Phys. Fluids* **24** 2163
[97] Swift J D and Schwar M J R 1970 *Electrical Probes for Plasma Diagnostics* (London: Iliffe)
[98] Riemann K-U 1991 *J. Phys. D: Appl. Phys.* **24** 493
[99] Tsendin L D and Golubovskii Y B 1977 *Sov. Phys.—Tech. Phys.* **22** 1066